Journal of
Breast Cancer **JBC**

Original Article

Check for updates

The Predictive Value of Magnetic Resonance Imaging-based Texture Analysis in Evaluating Histopathological Grades of Breast Phyllodes Tumor

Yifei Mao [1,*], **Zhongtang Xiong** [2,*], **Songxin Wu** [3], **Zhiqing Huang** [3], **Ruoxian Zhang** [3], **Yuqin He** [3], **Yuling Peng** [1], **Yang Ye** [1], **Tianfa Dong** [1], **Hui Mai** [1]

[1]Department of Radiology, The Third Affiliated Hospital of Guangzhou Medical University, Guangzhou, China
[2]Department of Pathology, The Third Affiliated Hospital of Guangzhou Medical University, Guangzhou, China
[3]Department of Radiology, Guangdong Women and Children Hospital, Guangzhou, China

OPEN ACCESS

Correspondence to
Tianfa Dong
Department of Radiology, The Third Affiliated Hospital of Guangzhou Medical University, No. 63 Duobao Road, Guangzhou 510150, China.
Email: 2019683078@gzhmu.edu.cn

Hui Mai
Department of Radiology, The Third Affiliated Hospital of Guangzhou Medical University, No. 63 Duobao Road, Guangzhou 510150, China.
Email: 2014683059@gzhmu.edu.cn

*Yifei Mao and Zhongtang Xiong have contributed equally to this work as co-first authors.

ORCID iDs
Yifei Mao
https://orcid.org/0000-0003-3766-1374
Zhongtang Xiong
https://orcid.org/0000-0003-0175-3138

ABSTRACT

Purpose: Knowing the distinction between benign and borderline/malignant phyllodes tumors (PTs) can help in the surgical treatment course. Herein, we investigated the value of magnetic resonance imaging-based texture analysis (MRI-TA) in differentiating between benign and borderline/malignant PTs.

Methods: Forty-three women with 44 histologically proven PTs underwent breast MRI before surgery and were classified into benign (n = 26) and borderline/malignant groups (n = 18 [15 borderline, 3 malignant]). Clinical and routine MRI parameters (CRMP) and MRI-TA were used to distinguish benign from borderline/malignant PT. In total, 298 texture parameters were extracted from fat-suppression (FS) T2-weighted, FS unenhanced T1-weighted, and FS first-enhanced T1-weighted sequences. To evaluate the diagnostic performance, receiver operating characteristic curve analysis was performed for the K-nearest neighbor classifier trained with significantly different parameters of CRMP, MRI sequence-based TA, and the combination strategy.

Results: Compared with benign PTs, borderline/malignant ones presented a higher local recurrence ($p = 0.045$); larger size ($p < 0.001$); different time-intensity curve pattern ($p = 0.010$); and higher frequency of strong lobulation ($p = 0.024$), septation enhancement ($p = 0.048$), cystic component ($p = 0.023$), and irregular cystic wall ($p = 0.045$). TA of FS T2-weighted images (0.86) showed a significantly higher area under the curve (AUC) than that of FS unenhanced T1-weighted (0.65, $p = 0.010$) or first-enhanced phase (0.72, $p = 0.049$) images. The texture parameters of FS T2-weighted sequences tended to have a higher AUC than CRMP (0.79, $p = 0.404$). Additionally, the combination strategy exhibited a similar AUC (0.89, $p = 0.622$) in comparison with the texture parameters of FS T2-weighted sequences.

Conclusion: MRI-TA demonstrated good predictive performance for breast PT pathological grading and could provide surgical planning guidance. Clinical data and routine MRI features were also valuable for grading PTs.

Keywords: Breast; Classification; Magnetic Resonance Imaging; Phyllodes Tumor

Songxin Wu
https://orcid.org/0000-0001-5830-2990
Zhiqing Huang
https://orcid.org/0000-0002-0598-3742
Ruoxian Zhang
https://orcid.org/0000-0002-7188-710X
Yuqin He
https://orcid.org/0000-0001-9954-7732
Yuling Peng
https://orcid.org/0000-0003-1942-4922
Yang Ye
https://orcid.org/0000-0001-5561-0103
Tianfa Dong
https://orcid.org/0000-0002-6654-513X
Hui Mai
https://orcid.org/0000-0001-9911-9519

INTRODUCTION

Phyllodes tumor (PT) is a unique type of fibroepithelial lesion that accounts for < 1% of all breast tumors [1]. According to the World Health Organization's (2012) 3-tiered classification, PTs are subcategorized into benign, borderline, or malignant based on several parameters, such as nuclear atypia, mitotic activity, stromal cellularity and overgrowth, and tumor margin [2]. According to a recent meta-analysis [3], the postoperative local recurrence rates in malignant, borderline, and benign PTs were 14%–21%, 11%–16%, and 6%–9%, respectively. Distant metastasis occurs in 10% of all patients with PT, mostly in malignant cases and in a few cases of borderline PT [4,5].

The National Comprehensive Cancer Network guidelines recommend local surgical excision with tumor-free margins of ≥ 1 cm, irrespective of grade for the treatment of PTs [6]. However, current evidence suggests that surgical options should also be selected according to the histologic grade [3,7,8]. Benign PTs can be treated conservatively because the margin status after excision is not significantly associated with local recurrence of benign PTs [3,7,8]. However, both borderline and malignant PTs require wide excision or mastectomy because a positive margin is significantly associated with higher rates of local recurrence [3,7,8]. Therefore, preoperative knowledge of the PT grade, especially distinguishing benign from borderline/malignant PTs, can potentially help in the surgical course of treatment and reduce operative complications caused by inadequate excision or unnecessary surgery.

Clinically, patients with benign PTs are usually younger than those with borderline/malignant PTs, and a larger tumor size is more suggestive of borderline/malignant PT. Compared with mammography and ultrasound, breast magnetic resonance imaging (MRI) has proven to be more valuable in the preoperative grading of PTs, as per previous reports [9,10]. Nevertheless, the overlap in clinical data and routine MRI characteristics between some benign and borderline/malignant PTs still poses some clinical challenges. Preoperative biopsy or intraoperative freezing is often difficult to assess accurately because of tumor tissue heterogeneity and insufficient sampling [11].

Previous MRI studies in PT grading mainly focused on the interpretation of MRI findings by visual and qualitative assessment of radiologists, with a lot of hidden information in the images remaining unused. Texture analysis (TA) is an emerging field that converts images into quantitative and mineable parameters that are imperceptible to the human eye [12]. Prior studies have demonstrated that TA can potentially be used in tumor grading by providing additional objective information on tumor heterogeneity [13-16]. Nonetheless, few studies have reported the predictive value of TA in the evaluation of the histological grade of breast PTs. Recently, Cui et al. [16] reported that TA could increase the predictive efficacy of mammography for the pathological grading of breast PTs.

With this background, our study aimed to investigate the value of MRI-based TA (hereafter, MRI-TA) to differentiate between benign and borderline/malignant PT and compare it with current clinical and routine MRI assessments.

METHODS

Patients

Initially, 58 consecutive female patients with histologically proven PT between April 2013 and April 2021 were retrospectively reviewed. The inclusion criteria were as follows: (1) after complete resection of the tumors, the specimens were diagnosed as PTs by 2 experienced pathologists and classified as benign, borderline, or malignant and (2) routine breast MRI performed 2 weeks prior to surgical excision. Patients were excluded based on the following conditions: (1) previous breast cancer diagnosis, (2) previous history of radiotherapy or chemotherapy, (3) vacuum-assisted breast biopsy performed before breast MRI, (4) poor image quality (artifacts or incomplete MRI sequences), and (5) tumors smaller than 1 cm (to reduce the unfavorable effects of small lesion size on radiological evaluation and TA). Finally, 43 female patients with 44 PTs (26 benign, 15 borderline, and 3 malignant PTs) met these criteria and were divided into the benign PT group (n = 26) and borderline/malignant PT group (n = 18). This study was approved by the institutional review board of The Third Affiliated Hospital of Guangzhou Medical University (approval number: 2021015). The need for written informed consent was waived by our institutional review board due to the retrospective nature of this study.

MRI acquisition

MRI examinations were performed using a 1.5-TMR scanner (Aurora Dedicated Breast MRI Systems; Aurora Healthcare, North Andover, USA) equipped with a single-channel breast coil before surgery in all patients. Dynamic enhanced imaging was performed using a transverse fat-suppression (FS) T1-weighted sequence in the axial plane (repetition time/echo time [TR/TE], 29.0/4.8 ms; slice thickness, 1.1 mm; matrix, 360 × 360 × 128; field of view [FOV], 36 cm). After acquisition of pre-contrast images, all patients were intravenously injected with 0.2 mL/kg body weight gadolinium-diethylenetriamine pentaacetic acid (Gd-DTPA, Magnevist; Schering AG, Berlin, Germany) at a rate of 2 mL/s, followed by the same rate of normal saline flush. Four post-contrast series were obtained at 90, 270, 450, and 630 seconds after the injection. Transverse FS T2-weighted maps (TR/TE, 6,680.0/68.0 ms; slice thickness, 3.0 mm; matrix, 320 × 192; FOV, 36 cm) were also generated.

Clinical and routine MRI evaluation

The clinical data and interpretations of breast MRI findings for each participant were defined as clinical and routine MRI parameters (CRMP) and applied to distinguish benign PT from borderline/malignant PT. Clinical data, including age, rapid enlargement, and primary/recurrence of lesions, were collected from medical records. Two radiologists (Yifei Mao and Hui Mai, with 6- and 13-years' MRI experience, respectively) blinded to the histopathological results, independently interpreted each MRI image. If the 2 radiologists had different opinions with respect to the interpretation of MRI findings, they reached a consensus through discussion. The following interpretations of each MRI scan were recorded: tumor size (the longest diameter on the first post-contrast sequence), margin (circumscribed vs. non-circumscribed), strong lobulation with an acute angle (present vs. absent), cystic component (present vs. absent), irregular cystic wall (present vs. absent), hypointense internal septation in FS T2-weighted sequences (present vs. absent), septation enhancement (present vs. absent), tumor signal in FS T2-weighted sequences (homogeneous vs. heterogeneous), kinetic curve assessment in the initial phase (slow, medium, or fast), and kinetic curve assessment in the delayed phase also called time-intensity curve pattern (persistent, plateau, or washout). Interpretation of margin and kinetic curve assessment

in the initial and delayed phases was based on the American College of Radiology Breast Imaging Reporting and Data System MRI criteria (2013) [17]. The area of the lesion where the enhancement was strongest in the first post-contrast image was chosen for kinetic curve assessment. To determine the presence of the cystic component and irregular cystic wall, we analyzed both unenhanced and enhanced images. **Figure 1** shows representative MR images. In this study, only clinical and MRI data before the first complete tumor resection at our institution were reviewed for patients with recurrence.

Texture analysis

TA of FS T2-weighted, FS unenhanced T1-weighted, and FS first-enhanced T1-weighted sequences was performed using MaZda software (version 4.6; Institute of Electronics, Technical University of Lodz, Lodz, Poland). Radiologist Yifei Mao chose representative image slices that contained the largest lesions. Then, regions of interest (ROIs) that covered the whole tumor with careful exclusion of the adjacent normal breast tissue were manually drawn. Radiologist Hui Mai reviewed the ROIs. In the event of disagreement, the 2 radiologists re-reviewed it to reach a consensus.

The ROIs of the MRI were normalized with the option of $\mu \pm 3\sigma$ (μ, gray-level mean; and σ, gray-level standard deviation [SD]) before computation of the texture parameters. The
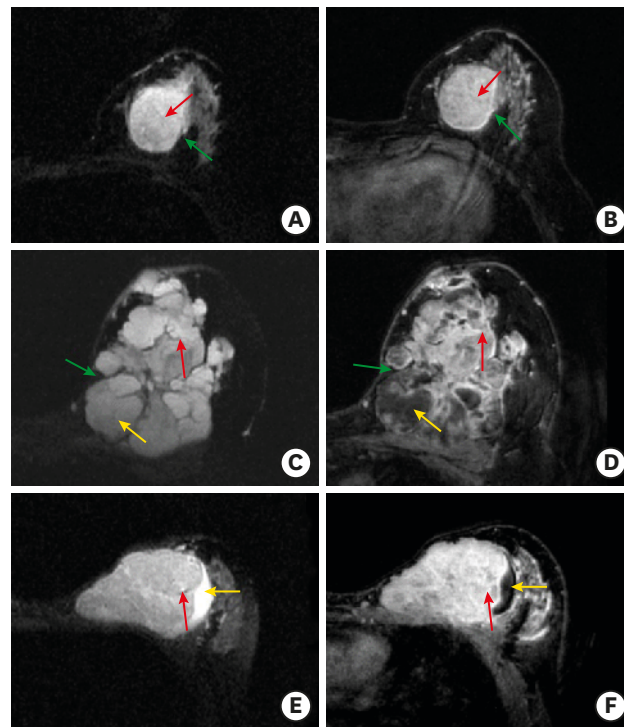
Figure 1. Representative magnetic resonance images. (A) Transverse FS T2-weighted and (B) FS-enhanced T1-weighted images from a patient with benign PT showing a mass with circumscribed margin, homogeneous signal in FS T2-weighted sequence, non-enhanced septation (red arrows), and non-strong lobulation (green arrows). (C) Transverse FS T2-weighted and (D) FS-enhanced T1-weighted images from a patient with borderline PT showing a mass with non-circumscribed margin, heterogeneous signal in FS T2-weighted sequence, enhanced septation (red arrows), strong lobulation (green arrows), and cystic component with irregular cystic wall (yellow arrows). (E) Transverse FS T2-weighted and (F) FS-enhanced T1-weighted images from a patient with malignant PT showing a lesion with non-circumscribed margin, heterogeneous signal in FS T2-weighted, enhanced septation (red arrows), and cystic component with regular cystic wall (yellow arrows).
FS = fat-suppression; PT = phyllodes tumor.
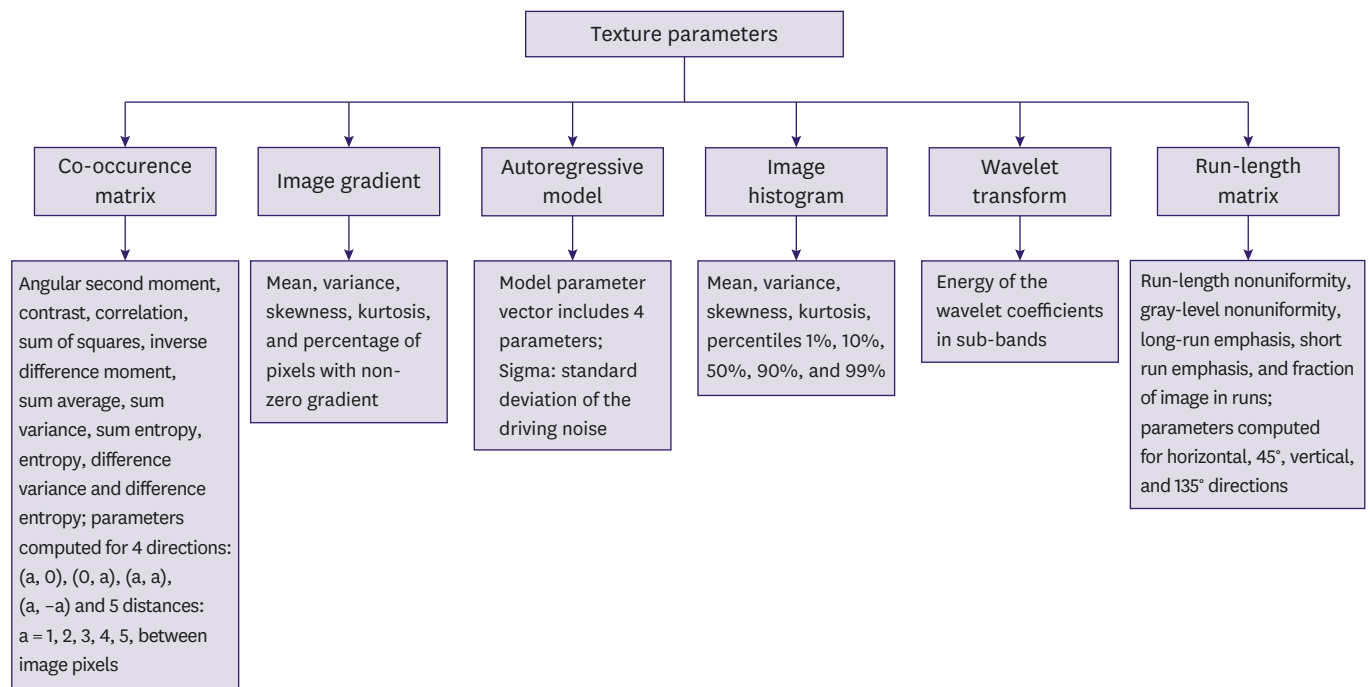
Figure 2. Summary of the texture parameters.

MaZda software provided an estimation of 298 texture parameters for each ROI [12,18]. The texture parameters are summarized in **Figure 2**. After computation of the parameters, 30 MRI-based texture parameters with the highest discriminative power for PT grading were determined using a parameter selection method based on a combination of the Fisher coefficient, classification error probability combined with average correlation coefficients, and mutual information.

Significantly different parameters ($p < 0.05$) were chosen from 30 MRI-based texture parameters with the highest discriminative power and CRMP for differentiation between benign and borderline/malignant PTs. These significantly different parameters were exported to the statistical program B11 in the MaZda software for further processing and classification [18]. A linear discriminant analysis was applied to reduce the parameter vector dimensions and increase discriminative power. The K-nearest neighbor classifier (K = 1) was used to distinguish benign PT from borderline or malignant PT based on the most discriminative parameters after linear discriminant analysis. All lesion classifications were performed after standardization of the parameters. **Figure 3** presents a flowchart illustrating how CRMP and texture parameters on MRI sequences were chosen for PT grading.

Statistical analyses

The texture parameters with the highest discriminative power and CRMP were analyzed using the Mann-Whitney U test, χ^2 test, and Fisher's exact test, as appropriate, and the significantly different parameters ($p < 0.05$) between benign and borderline/malignant PTs were chosen. To evaluate the diagnostic performance of each approach, receiver operating characteristic (ROC) analyses were performed for the K-nearest neighbor classifier trained with significantly different parameters of CRMP, MRI-TA, and the combination strategy. Statistical analyses were performed using IBM Statistical Package for the Social Sciences
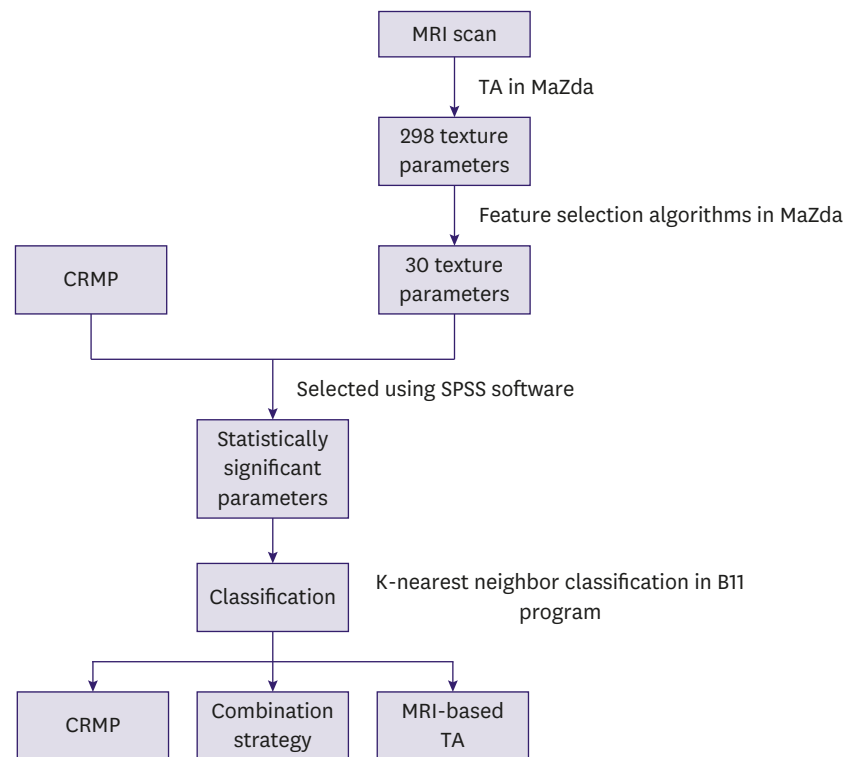
Figure 3. A flowchart illustrating how the clinical and routine MRI parameters and texture parameters on MRI sequences were chosen for phyllodes tumor grading.
MRI = magnetic resonance imaging; TA = texture analysis; CRMP = clinical and routine magnetic resonance imaging parameters; MRI-TA = magnetic resonance imaging-based texture analysis.

(version 22.0; IBM Corporation, Armonk, USA) and the R software package (version 4.0.3; The R Foundation for Statistical Computing, Vienna, Austria). Statistical significance was set at $p < 0.05$.

RESULTS

Clinical and routine MRI parameters

Table 1 presents the clinical data and routine MRI parameters of PTs. The mean age (mean ± SD) was 43.73 ± 6.09 for the benign PTs and 45.94 ± 7.42 for the borderline/malignant PTs. There were 32 primary and 12 recurrent PTs. Borderline/malignant PTs had a significantly higher local recurrence rate than benign tumors (44.4% [8/18] vs. 15.4% [4/26], $p = 0.045$). The tumor size (mean ± SD) was 3.32 ± 2.21 cm for benign PTs and 6.76 ± 4.02 cm for borderline/malignant tumors. Tumors in the benign PT group were smaller than those in the borderline/malignant PT group ($p < 0.001$). Overall, 83.3% (15/18) of borderline/malignant PTs showed strong lobulation, while only half (13/26) of the benign tumors showed strong lobulation. A strong lobulation pattern was more common in borderline/malignant tumors than in benign ones ($p = 0.024$). Septation enhancement was observed in 33.3% (6/18) of borderline/malignant PTs and 7.7% (2/26) of benign tumors with statistically significant differences ($p = 0.048$). Cystic components were observed in 11 of 18 (61.1%) borderline/malignant PTs, but only in 7 of 26 (26.9%) benign tumors ($p = 0.023$). Compared with benign PTs, borderline/malignant PTs had a significantly higher frequency of irregular cystic walls (p

Table 1. Summary of clinical and routine MRI parameters of phyllodes tumors

Characteristics	Benign (n = 26)	Borderline & malignant (n = 18)	p-value
Mean age	43.73 ± 6.09	45.94 ± 7.42	0.218[*]
Rapid enlargement			0.831[†]
Absent	18 (69.2)	13 (72.2)	
Present	8 (30.8)	5 (27.8)	
Primary/Recurrence			0.045[‡]
Primary	22 (84.6)	10 (55.6)	
Recurrence	4 (15.4)	8 (44.4)	
Diameter	3.32 ± 2.21	6.76 ± 4.02	< 0.001[*]
Margin			0.273[‡]
Circumscribed	22 (84.6)	12 (66.7)	
Not circumscribed	4 (15.4)	6 (33.3)	
Strong lobulation			0.024[†]
Absent	13 (50.0)	3 (16.7)	
Present	13 (50.0)	15 (83.3)	
Hypointense septation			0.105[†]
Absent	12 (46.2)	4 (22.2)	
Present	14 (53.8)	14 (77.8)	
Septation enhancement			0.048[‡]
Absent	24 (92.3)	12 (66.7)	
Present	2 (7.7)	6 (33.3)	
Cystic component			0.023[†]
Absent	19 (73.1)	7 (38.9)	
Present	7 (26.9)	11 (61.1)	
Irregular cystic wall			0.045[‡]
Absent	22 (84.6)	10 (55.6)	
Present	4 (15.4)	8 (44.4)	
FS T2-weighted sequence			0.263[†]
Homogeneous	16 (61.5)	8 (44.4)	
Heterogeneous	10 (38.5)	10 (55.6)	
Initial enhancement			0.063[‡]
Slow	3 (11.5)	1 (5. 5)	
Medium	12 (46.2)	3 (16.7)	
Fast	11 (42.3)	14 (77.8)	
TIC pattern			0.010[‡]
Persistent pattern	12 (46.2)	7 (38.9)	
Plateau pattern	13 (50)	4 (22.2)	
Washout pattern	1 (3.8)	7 (38.9)	

Values are presented as mean ± standard deviation or number (%).
MRI = magnetic resonance imaging; FS = fat-suppression; TIC = time-intensity curve.
[*]Mann-Whitney *U* test; [†]Chi-square test; [‡]Fisher's exact test.

= 0.045). The time-intensity curve pattern was significantly different between the 2 groups of PTs (p = 0.010). Borderline/malignant PTs had a higher frequency of washout pattern (38.9% [7/18] vs. 3.8% [1/26]) and a lower frequency of persistent (38.9% [7/18] vs. 46.2% [12/26]) and plateau (22.2% [4/18] vs. 50.0% [13/26]) enhancement than benign PTs.

No significant differences were observed between benign and borderline/malignant PTs with respect to age, rapid enlargement, margins, hypointense internal septation and tumor signal intensity in FS T2-weighted sequences, and kinetic curve assessment in the initial phase.

For clinical characteristics and routine MRI findings, the K-nearest neighbor classifier had a classification accuracy of 79.5% (35/44). ROC analysis showed that the area under the curve (AUC) was 0.79 (95% CI, 0.65–0.94), and the sensitivity and specificity were 77.8% (14/18) and 80.8% (21/26), respectively.

Texture parameters

Different PT grades presented different textural patterns. FS T2-weighted, FS unenhanced T1-weighted, and FS first-enhanced T1-weighted sequences had 25, 23, and 20 statistically significant texture parameters, respectively. The significant texture parameters of benign and borderline/malignant PTs are presented in **Table 2** and **Supplementary Tables 1** and **2**. The K-nearest neighbor classifier had 86.4% (38/44), 65.9% (29/44), and 72.7% (32/44) classification accuracy for FS T2-weighted, FS unenhanced T1-weighted, and first-enhanced phase sequences, respectively. ROC analysis showed that the AUCs were 0.86 (95% CI, 0.74–0.98), 0.65 (95% CI, 0.48–0.82), and 0.72 (95% CI, 0.56–0.88) for FS T2-weighted, FS unenhanced T1-weighted, and FS first-enhanced T1-weighted images, respectively. The statistically different texture parameters of FS T2-weighted images showed a significantly higher AUC than those of FS unenhanced T1-weighted (0.86 [95% CI, 0.74–0.98] vs. 0.65 [95% CI, 0.48–0.82], $p = 0.010$) or first-enhanced phase (0.86 [95% CI, 0.74–0.98] vs. 0.72 [95% CI, 0.56–0.88], $p = 0.049$) images. The classification performance results are listed in **Table 3**.

Table 2. Statistically significant texture parameters on transverse fat-suppression T2-weighted images

Texture parameters	p	Z
WavEnLL_s-1	0.007	−2.72
45dgr_GLevNonU	0.003	−2.98
S(5,−5)Correlat	0.003	−2.96
S(5,−5)Contrast	0.004	−2.86
S(0,5)DifVarnc	0.005	−2.84
S(0,5)Correlat	0.011	−2.55
S(4,−4)DifVarnc	0.005	−2.84
S(4,−4)SumVarnc	0.008	−2.67
S(4,−4)InvDfMom	0.008	−2.67
S(4,−4)Correlat	0.003	−3.01
S(4,−4)Contrast	0.003	−3.10
S(0,4)DifVarnc	0.005	−2.79
S(0,4)Correlat	0.011	−2.53
S(0,4)Contrast	0.010	−2.58
S(3,−3)DifEntrp	0.005	−2.79
S(3,−3)DifVarnc	0.005	−2.82
S(3,−3)Correlat	0.005	−2.84
S(3,−3)Contrast	0.002	−3.06
S(0,3)DifVarnc	0.008	−2.67
S(2,−2)DifEntrp	0.004	−2.86
S(2,−2)SumAverg	0.003	−2.96
S(0,2)DifVarnc	0.019	−2.34
S(1,−1)DifEntrp	0.009	−2.63
S(1,−1)SumAverg	0.005	−2.79
Perc.01%	0.040	−2.05

Table 3. Classification performances and receiver operating characteristic analysis of phyllodes tumors grading

Characteristics	Classification accuracy (%)	AUC (95% CI)	Sensitivity (%)	Specificity (%)
FS T2-weighted	86.4 (38/44)	0.86 (0.74–0.98)	83.3 (15/18)	88.5 (23/26)
FS-unenhanced T1-weighted	65.9 (29/44)	0.65 (0.48–0.82)	61.1 (11/18)	69.2 (18/26)
First enhanced T1-weighted	72.7 (32/44)	0.72 (0.56–0.88)	66.7 (12/18)	76.9 (20/26)
CRMP	79.5 (35/44)	0.79 (0.65–0.94)	77.8 (14/18)	80.8 (21/26)
Combination strategy	88.6 (39/44)	0.89 (0.78–1.00)	88.9 (16/18)	88.5 (23/26)

AUC = area under the curve; CI = confidence interval; FS = fat-suppression; CRMP = clinical and routine magnetic resonance imaging parameters.
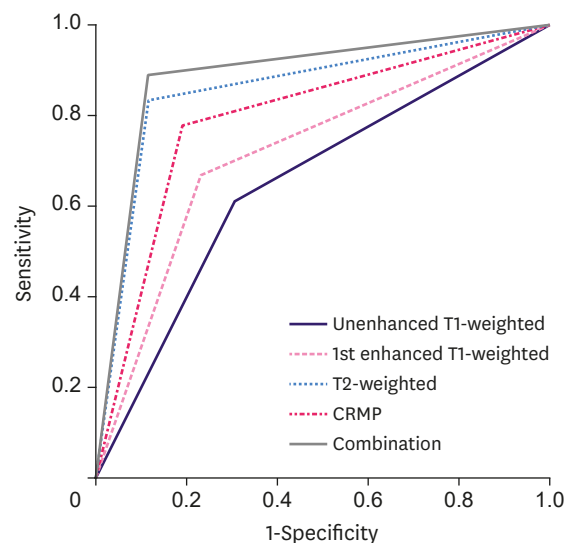
Combination strategy

By combining the CRMP and texture parameters of FS T2-weighted images, the classification accuracy was 88.6% (39/44) and the AUC was 0.89 (95% CI, 0.78–1.00) with a sensitivity and specificity of 88.9% (16/18) and 88.5% (23/26), respectively, for differentiating between benign and borderline/malignant PTs.

Diagnostic performance

The ROC curves for CRMP, MRI-TA, and the combination strategy were compared to assess the diagnostic performance of each strategy (**Figure 4** and **Table 3**). The texture parameters of FS T2-weighted sequences appeared to have a higher classification accuracy (86.4% [38/44] vs. 79.5% [35/44]) and higher AUC (0.86 [95% CI, 0.74–0.98] vs. 0.79 [95% CI, 0.65–0.94]) than CRMP. However, no statistically significant differences in AUC were observed between TA based on any MRI series and CRMP (p = 0.404, 0.129, and 0.408 for texture parameters of FS T2-weighted, FS unenhanced T1-weighted, and first-enhanced sequences, respectively). The texture parameters of FS T2-weighted sequences tended to be more sensitive (83.3% [15/18] vs. 77.8% [14/18]) and specific (88.5% [23/26] vs. 80.8% [21/26]) than those on CRMP. Owing to the overlapping effect of CRMP, 4 borderline/malignant PTs were misinterpreted as benign (**Figure 5**) and 5 benign PTs were mistakenly interpreted as borderline/malignant (**Figure 6**). The combination strategy tended to have a higher classification accuracy (88.6% [39/44] vs. 79.5% [35/44]) and higher (although not significant) AUC (0.89 [95% CI, 0.78–1.00] vs. 0.79 [95% CI, 0.65–0.94], p = 0.232) than CRMP alone for differentiating between benign and borderline/malignant PTs. In addition, the combination strategy exhibited similar performance in terms of classification accuracy (88.6% [39/44] vs. 86.4% [38/44]), AUC (0.89 [95% CI, 0.78–1.00] vs. 0.86 [95% CI, 0.74–0.98], p = 0.622), specificity (88.5% [23/26] vs. 88.5% [23/26]), and sensitivity (88.9% [16/18] vs. 83.3% [15/18]) compared to the texture parameters of FS T2-weighted sequences.

Figure 4. Performances of the clinical and routine MRI parameters, texture parameters from MRI sequences, and combination strategy for phyllodes tumor grading are illustrated with receiver operating characteristic curves. MRI = magnetic resonance imaging; CRMP = clinical and routine magnetic resonance imaging parameters.
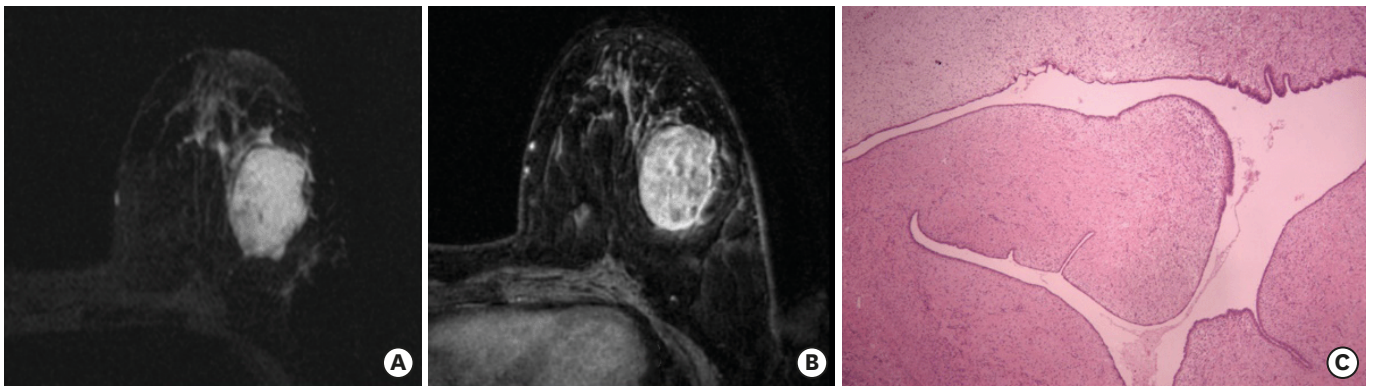
Figure 5. A borderline PT in a 52-year-old woman (A) transverse FS T2-weighted image, (B) FS-enhanced T1-weighted image, (C) pathological image (hematoxylin and eosin: 100× magnification). The texture parameters of FS T2-weighted sequence correctly identified a borderline/malignant PT that was falsely classified as a benign PT based on clinical and routine MRI parameters, possibly because of the absence of strong lobulation, cystic area, and enhanced septation.
PT = phyllodes tumor; FS = fat-suppression; MRI = magnetic resonance imaging.
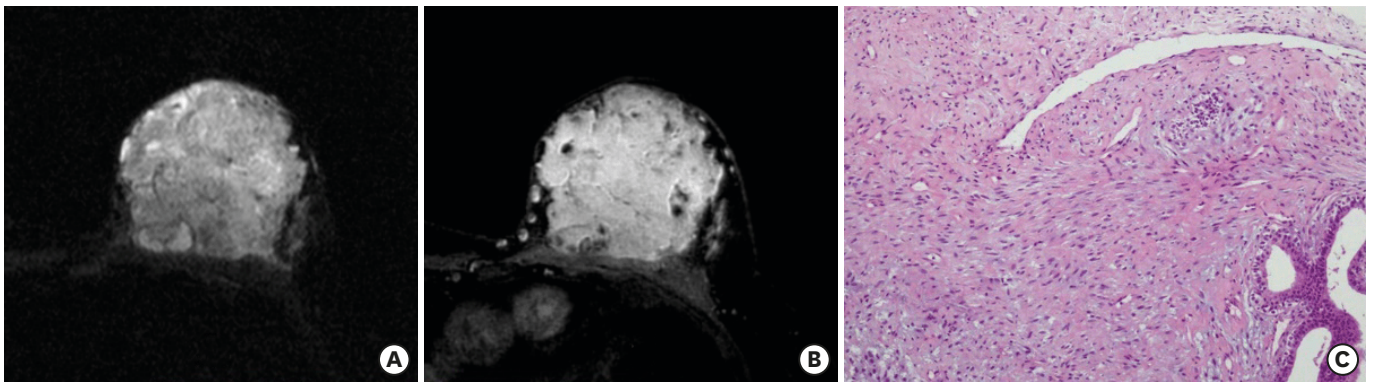
Figure 6. A benign PT in a 49-year-old woman (A) transverse FS T2-weighted image (B) FS-enhanced T1-weighted image, and (C) pathological image (hematoxylin and eosin: 200× magnification). The texture parameters of FS T2-weighted sequence correctly identified benign PT that was falsely classified as a borderline/malignant PT on clinical and routine MRI parameters, possibly because of the large size, non-circumscribed margin, strong lobulation, heterogeneous signal in FS T2-weighted sequence, cystic area with irregular cystic wall, and enhanced septation.
PT = phyllodes tumor; FS = fat-suppression; MRI = magnetic resonance imaging.

DISCUSSION

The texture parameters of FS T2-weighted sequences performed well in distinguishing benign from borderline/malignant PTs with high classification accuracy (86.4% [38/44]), AUC (0.86; 95% CI, 0.74–0.98), sensitivity (83.3% [15/18]), and specificity (88.5% [23/26]). Although there was no significant difference in the AUC between the texture parameters of FS T2-weighted sequences and CRMP, a trend towards better grading performance using the texture parameters of FS T2-weighted sequences was noted. In addition, a comparison of the combination strategy and texture parameters of FS T2-weighted sequences alone revealed that both the approaches showed similar performance for differentiating between benign and borderline/malignant PTs.

MRI has proven to be more valuable than both mammography and ultrasound in PT grading [9,10]. Previous studies have proven that some clinical parameters and routine MRI findings are useful in grading breast PTs, which is largely consistent with our findings but with certain differences. The present study showed that tumor size in the borderline/malignant PT group was significantly larger than that in the benign group ($p < 0.05$), which is consistent with

previous study results in that the likelihood of malignancy increased with increasing tumor size [11,19,20]. This is likely attributed to the greater proliferative activity in high-grade PTs than in low-grade ones. A strong lobulation pattern was presented more frequently in borderline/malignant PTs than in benign ones ($p < 0.05$), which is consistent with a previous mammogram-based study of PT [16]. Tan et al. [10] reported that hypointense internal septation in T2-weighted images is associated with the histologic grade of PTs. However, in our study, significant differences were found in septation enhancement but not in the hypointense internal septation between benign and borderline/malignant PTs. Septation enhancement has rarely been reported in previous studies. We suspected that the internal septation enhancement was related to cellular atypia of the tumor tissue. Additionally, in our study, both cystic area and irregular cystic wall were more frequently observed in the borderline/malignant PT group than in the benign PT group ($p < 0.05$), which means that cystic change, especially with an irregular cystic wall, is valuable for differentiating benign from borderline/malignant PTs. This is consistent with the results reported by Yabuuchi et al. [9]. The presence of irregular cystic walls corresponded histologically to necrosis. The higher the degree of malignancy, the faster the tumor growth and the easier the path to necrosis.

Yabuuchi et al. [9] suggested that the enhancement pattern is not necessarily helpful in predicting the histological grade of PTs. However, based on our data, borderline/malignant PTs presented a significantly higher frequency of washout patterns than benign PTs. These differences may be related to the sample size and different group strategies: in their study, 2 enhancement patterns (plateau/washout and persistent) were compared among 3 grades of PT (benign, borderline, malignant), while 3 enhancement patterns (plateau, washout, persistent) were compared between benign and borderline/malignant PTs in ours. The expression of stromal vascular endothelial growth factor in PTs increases with an increase in the degree of malignancy [21], inducing increased tumor-associated angiogenesis. Increased vascularity (vessel density) with a pathological vessel wall architecture increases vascular permeability [22-24]. In addition, the interstitial cells of borderline/malignant PTs are more abundant, dense, and overgrown [2]; hence, the extravascular extracellular space (EES) is relatively small. Gd-DTPA is an extracellular contrast agent. Increased vascular permeability and smaller EES lead to a lower presence of Gd-DTPA in the EES and quicker clearance of Gd-DTPA from the EES in borderline/malignant PTs, reflecting a rapid signal decrease during the delayed phase. This may explain the higher frequency of washout patterns in borderline/malignant PTs.

It is noteworthy that in our study, benign PTs showed overlapping MRI parameters with borderline/malignant PTs. Some large benign PTs with abundant blood supply may be misdiagnosed as borderline/malignant PTs, resulting in false-positive results. Borderline/malignant PTs with a small size or unabundant blood supply could be mistaken for benign PTs, which tends to produce false-negative results.

The FS T2-weighted sequence revealed more statistically significant texture parameters than the FS unenhanced T1-weighted and first-enhanced T1-weighted sequences. Moreover, the predictive performance of statistically significant texture parameters of FS T2-weighted images was better than that of statistically significant texture parameters in other MRI series. Prior breast MRI studies [14,25,26] using TA have focused on dynamic contrast-enhanced sequences, probably owing to their hemodynamic information. Our study showed that texture parameters calculated from FS T2-weighted sequences, which were often neglected previously, also played an important role in PT grading assessment. Benefiting from the relatively long echo time of an FS T2-weighted sequence, a higher signal-to-noise ratio,

spatial resolution, and soft-tissue contrast of different grades of PTs can be achieved. Thus, statistically significant texture parameters derived from FS T2-weighted sequences might reflect more information regarding the heterogeneity of the tumor microenvironment and, in turn, could provide better grading performance in distinguishing benign from borderline/malignant PTs.

Heterogeneity of tumor reflects the regional differences in tumor cellularity, proliferation, angiogenesis, and necrosis [27,28], all of which are associated with tumor grade. The texture parameters extracted from medical images allow objective evaluation of tumor heterogeneity [14,29,30], suggesting the potential use of TA in tumor grading. Cui et al. [16] found that the AUC of mammographic findings was higher than that of mammographic TA and lower than that of the combination strategy in differentiating benign from borderline/malignant PTs, but no ROC comparison was performed. Similar to the results of our study, their results demonstrated that TA is useful in PT grading, but could not reach a firm conclusion about TA outperforming radiographic findings.

Our study had several limitations. First, the small sample size is the main limitation of our study. The results of our study should take into consideration that our analysis was restricted to a small sample size. Second, the number of borderline and malignant PTs was relatively small; therefore, we combined borderline and malignant PTs into a single group for comparison with the benign PT group. Third, a small number of MRI images in this study were collected after puncture biopsy, which might have caused local bleeding or edema within the tumor, thereby affecting the assessment of certain parameters. Fourth, the pathophysiological semantics of some texture parameters are poorly understood at present; therefore, further study is needed to understand the underlying pathophysiological information of tumors reflected by different texture parameters. Finally, the inherent bias of this retrospective study design must be acknowledged. Future studies with larger datasets are needed to validate our results.

In our study, MRI-TA demonstrated good predictive performance for breast PT pathological grading. Clinical data and routine MRI features were also valuable for grading PTs. MRI-TA alone could not substitute radiologists in the diagnosis of PT grades, but it could provide guidance for the selection of operation plans prior to surgery.

ACKNOWLEDGMENTS

SUPPLEMENTARY MATERIALS

Supplementary Table 1
Statistically significant texture parameters on transverse fat-suppression unenhanced T1-weighted images

Click here to view

Supplementary Table 2
Statistically significant texture parameters on transverse fat-suppression first enhanced T1-weighted images

Click here to view

REFERENCES

1. Liberman L, Bonaccio E, Hamele-Bena D, Abramson AF, Cohen MA, Dershaw DD. Benign and malignant phyllodes tumors: mammographic and sonographic findings. Radiology 1996;198:121-4.
   PUBMED | CROSSREF

2. Frank GA, Danilova NV, Andreeva IIu, Nefedova NA. WHO classification of tumors of the breast, 2012. Arkh Patol 2013;75:53-63.
   PUBMED

3. Lu Y, Chen Y, Zhu L, Cartwright P, Song E, Jacobs L, et al. Local recurrence of benign, borderline, and malignant phyllodes tumors of the breast: a systematic review and meta-analysis. Ann Surg Oncol 2019;26:1263-75.
   PUBMED | CROSSREF

4. Park HJ, Ryu HS, Kim K, Shin KH, Han W, Noh DY. Risk factors for recurrence of malignant phyllodes tumors of the breast. In Vivo 2019;33:263-9.
   PUBMED | CROSSREF

5. Zhang Y, Kleer CG. Phyllodes tumor of the breast: histopathologic features, differential diagnosis, and molecular/genetic updates. Arch Pathol Lab Med 2016;140:665-71.
   PUBMED | CROSSREF

6. Gradishar WJ, Anderson BO, Abraham J, Aft R, Agnese D, Allison KH, et al. Breast cancer, version 3.2020, NCCN clinical practice guidelines in oncology. J Natl Compr Canc Netw 2020;18:452-78.
   PUBMED | CROSSREF

7. Lim RS, Cordeiro E, Lau J, Lim A, Roberts A, Seely J. Phyllodes tumors-the predictors and detection of recurrence. Can Assoc Radiol J 2021;72:251-7.
   PUBMED | CROSSREF

8. Noordman PC, Klioueva NM, Weimann MN, Borgstein PJ, Vrouenraets BC. Phyllodes tumors of the breast: a retrospective analysis of 57 cases. Breast Cancer Res Treat 2020;181:361-7.
   PUBMED | CROSSREF

9. Yabuuchi H, Soeda H, Matsuo Y, Okafuji T, Eguchi T, Sakai S, et al. Phyllodes tumor of the breast: correlation between MR findings and histologic grade. Radiology 2006;241:702-9.
   PUBMED | CROSSREF

10. Tan H, Zhang S, Liu H, Peng W, Li R, Gu Y, et al. Imaging findings in phyllodes tumors of the breast. Eur J Radiol 2012;81:e62-9.
    PUBMED | CROSSREF

11. Foxcroft LM, Evans EB, Porter AJ. Difficulties in the pre-operative diagnosis of phyllodes tumours of the breast: a study of 84 cases. Breast 2007;16:27-37.
    PUBMED | CROSSREF

12. Castellano G, Bonilha L, Li LM, Cendes F. Texture analysis of medical images. Clin Radiol 2004;59:1061-9.
    PUBMED | CROSSREF

13. Oh J, Lee JM, Park J, Joo I, Yoon JH, Lee DH, et al. Hepatocellular carcinoma: texture analysis of preoperative computed tomography images can provide markers of tumor grade and disease-free survival. Korean J Radiol 2019;20:569-79.
    PUBMED | CROSSREF

14. Nie K, Chen JH, Yu HJ, Chu Y, Nalcioglu O, Su MY. Quantitative analysis of lesion morphology and texture features for diagnostic prediction in breast MRI. Acad Radiol 2008;15:1513-25.
    PUBMED | CROSSREF

15. Mai H, Mao Y, Dong T, Tan Y, Huang X, Wu S, et al. The utility of texture analysis based on breast magnetic resonance imaging in differentiating phyllodes tumors from fibroadenomas. Front Oncol 2019;9:1021.
    PUBMED | CROSSREF

16. Cui WJ, Wang C, Jia L, Ren S, Duan SF, Cui C, et al. Differentiation between G1 and G2/G3 phyllodes tumors of breast using mammography and mammographic texture analysis. Front Oncol 2019;9:433.
PUBMED | CROSSREF

17. American College of Radiology. Breast Imaging Reporting and Data System (BIRADS Atlas) MRI-Lexicon. 5th ed. Reston: American College of Radiology; 2013.

18. Szczypiński PM, Strzelecki M, Materka A, Klepaczko A. MaZda--a software package for image texture analysis. Comput Methods Programs Biomed 2009;94:66-76.
PUBMED | CROSSREF

19. Komenaka IK, El-Tamer M, Pile-Spellman E, Hibshoosh H. Core needle biopsy as a diagnostic tool to differentiate phyllodes tumor from fibroadenoma. Arch Surg 2003;138:987-90.
PUBMED | CROSSREF

20. Bode MK, Rissanen T, Apaja-Sarkkinen M. Ultrasonography and core needle biopsy in the differential diagnosis of fibroadenoma and tumor phyllodes. Acta Radiol 2007;48:708-13.
PUBMED | CROSSREF

21. Tse GM, Lui PC, Lee CS, Kung FY, Scolyer RA, Law BK, et al. Stromal expression of vascular endothelial growth factor correlates with tumor grade and microvessel density in mammary phyllodes tumors: a multicenter study of 185 cases. Hum Pathol 2004;35:1053-7.
PUBMED | CROSSREF

22. Pham CD, Roberts TP, van Bruggen N, Melnyk O, Mann J, Ferrara N, et al. Magnetic resonance imaging detects suppression of tumor vascular permeability after administration of antibody to vascular endothelial growth factor. Cancer Invest 1998;16:225-30.
PUBMED | CROSSREF

23. Buckley DL, Drew PJ, Mussurakis S, Monson JR, Horsman A. Microvessel density of invasive breast cancer assessed by dynamic Gd-DTPA enhanced MRI. J Magn Reson Imaging 1997;7:461-4.
PUBMED | CROSSREF

24. Buadu LD, Murakami J, Murayama S, Hashiguchi N, Sakai S, Masuda K, et al. Breast lesions: correlation of contrast medium enhancement patterns on MR images with histopathologic findings and tumor angiogenesis. Radiology 1996;200:639-49.
PUBMED | CROSSREF

25. Amano Y, Woo J, Amano M, Yanagisawa F, Yamamoto H, Tani M. MRI texture analysis of background parenchymal enhancement of the breast. Biomed Res Int 2017;2017:4845909.
PUBMED | CROSSREF

26. Liu C, Ding J, Spuhler K, Gao Y, Serrano Sosa M, Moriarty M, et al. Preoperative prediction of sentinel lymph node metastasis in breast cancer by radiomic signatures from dynamic contrast-enhanced MRI. J Magn Reson Imaging 2019;49:131-40.
PUBMED | CROSSREF

27. Cook GJ, Yip C, Siddique M, Goh V, Chicklore S, Roy A, et al. Are pretreatment ^{18}F-FDG PET tumor textural features in non-small cell lung cancer associated with response and survival after chemoradiotherapy? J Nucl Med 2013;54:19-26.
PUBMED | CROSSREF

28. Ganeshan B, Goh V, Mandeville HC, Ng QS, Hoskin PJ, Miles KA. Non-small cell lung cancer: histopathologic correlates for texture parameters at CT. Radiology 2013;266:326-36.
PUBMED | CROSSREF

29. Kim JH, Ko ES, Lim Y, Lee KS, Han BK, Ko EY, et al. Breast cancer heterogeneity: MR imaging texture analysis and survival outcomes. Radiology 2017;282:665-75.
PUBMED | CROSSREF

30. Ko ES, Kim JH, Lim Y, Han BK, Cho EY, Nam SJ. Assessment of invasive breast cancer heterogeneity using whole-tumor magnetic resonance imaging texture analysis: correlations with detailed pathological findings. Medicine (Baltimore) 2016;95:e2453.
PUBMED | CROSSREF